

# Cover cracking in RC columns subjected to reinforcement corrosion under sustained load

S. Jabbour

*Halsall Associates Limited, and University of Ottawa, Canada*

B. Martín-Pérez

*University of Ottawa, Ontario, Canada*

**ABSTRACT:** This paper presents the results of an experimental study wherein circular spirally-reinforced concrete columns were subjected to accelerated corrosion while sustaining a constant service compressive load. Two types of specimens were used in the experimental program: type CV, where vertical reinforcement was corroded and isolated from non-confining spiral reinforcement, and type CS where spiral reinforcement was corroded and isolated from the vertical reinforcement to study the effect of confinement. The cracking initiation, pattern, and widening of the concrete cover were monitored for ten months, and relations obtained between the crack widening and propagation and the elastic shortening of the column and steel mass loss were established. The cracking pattern was found to be wider and in the form of longitudinal cracks along the vertical bars in type CV columns, but more random and distributed over the surface and not as wide in type CS columns.

## 1 INTRODUCTION

One of the major causes of deterioration of North American reinforced concrete (RC) infrastructure today is corrosion of the reinforcement. The extensive use of de-icing salts on highways in the winter time brings to the concrete surface an excessive supply of chloride ions, which penetrate the concrete cover and eventually destroy the passive layer that protects the reinforcement from corrosion. The break-down of this passive layer, which is a film that forms around the reinforcement due to the high alkalinity of concrete and reduces the corrosion to negligible levels, leads to the initiation of the corrosion process. The accumulation of corrosion products around the reinforcement results in expansive forces which, once they exceed the tensile strength of concrete cover, lead to cracking of the concrete surface. The cracking of the concrete cover initiates a degradation process that worsens with the propagation of corrosion and eventually leads to further deterioration in the form of delamination and spalling of the concrete cover.

The main corrosion-induced damage mechanisms in RC are: (i) the decrease in the reinforcement cross-sectional area, (ii) the possible loss of steel ductility, (iii) the cracking and spalling of the concrete cover, and (iv) the loss of bond along the steel/concrete interface. There has been an increasing effort in recent years to quantify the damage pro-

gress in RC due to the advance of steel reinforcement corrosion. Particularly, quantifying concrete cracking propagation with respect to reinforcement corrosion propagation is of great relevance in the serviceability assessment of deteriorated RC structures with corroded reinforcement, and it must be included in estimations of residual service life (Andrade & Alonso 1996, Liu & Weyers 1998).

There have been limited studies on the effect of reinforcement corrosion on the serviceability and structural performance of RC columns (Lee et al. 2000, Rodriguez et al. 1996, Saito et al. 2007). A major observation from these studies is that the load carrying capacity of corroded columns is lower than that of non-corroded columns. This reduction in resistance capacity is attributed to: (a) the increase in load eccentricity due to uneven corrosion of the longitudinal reinforcement; (b) buckling of the longitudinal reinforcing bars when column ties are corroded; and, (c) the actual deterioration of the concrete section due to cracking, spalling and/or delamination of the concrete cover. However, none of the above studies were conducted on RC columns that were subjected to sustained axial loads and reinforcement corrosion simultaneously.

This paper presents the results of an experimental program in which ten RC circular columns were subjected to accelerated reinforcement corrosion while sustaining in-service loads. The objective of this research was to investigate the simultaneous effect of

in-service load and corrosion-induced damage on RC column serviceability. To that end, crack initiation and propagation as well as longitudinal and circumferential deformation were monitored during testing.

## 2 EXPERIMENTAL PROGRAM

### 2.1 Test specimens

The RC column specimens used in this study consist of a 260-mm diameter circular cross-section reinforced with 6-15M longitudinal bars ( $\phi = 16.0$  mm) and 10M spirals ( $\phi = 11.3$  mm). The concrete cover to spiral reinforcement was 20 mm. The cross-section of the columns is illustrated in Figure 1. The compressive strength of concrete used in the design was 25 MPa, and the steel yield strength used was 400 MPa. Two types of column designs were used in the experimental investigation, with five specimens of each type being built. The difference between the two designs was the spacing of the spiral reinforcement, which was specified to 220 mm for type CV columns, and 80 mm for type CS columns, respectively. The difference in spiral pitch allowed investigating the effect of confinement on the behaviour of corroded columns. Figure 2 shows the reinforcement cage used in the RC specimens.

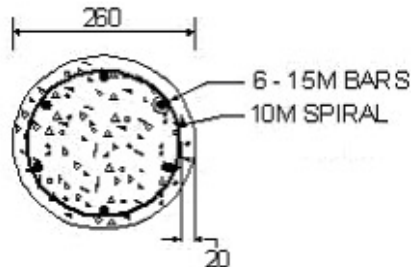


Figure 1. Details of RC columns' cross-section.

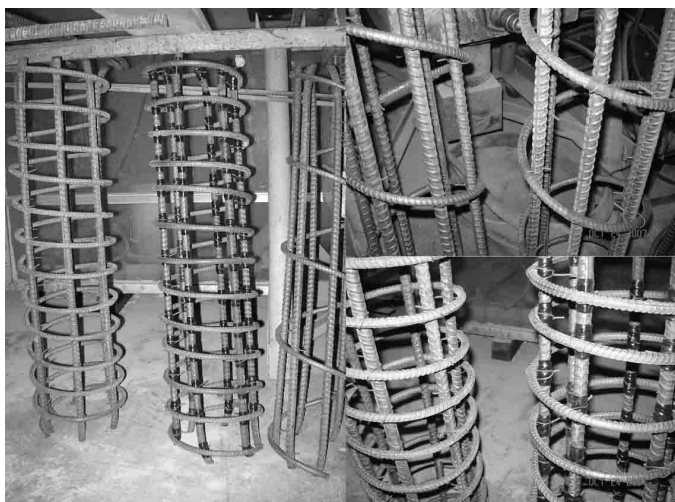


Figure 2. Reinforcement cage used in RC columns.

Column ends were further confined with twelve-mm thick steel collars, in order to limit damage

propagation to the middle zone of the column instead of at anchorage regions. Each cap plate had four 300-mm long anchors bent at their ends to allow application of eccentric loading through the cap plates in future testing. High-strength non-shrink grout was used for a depth of 50 mm at both ends of the column to make sure the columns were fully adhered to their caps at casting. The steel caps as well as other steel accessories were all painted with zinc-based protective coating in order to minimize the propagation of corrosion outside the columns reinforcement.

Since concrete properties are crucial in determining the rate and nature of future propagation of corrosion and the amount of corrosion-induced cracking, the material quantities and properties of the concrete mix used in the experimental work were carefully examined. The concrete mix design was decided based on two main concepts: (i) a practical realistic concrete compressive strength was used to represent a real life situation, and (ii) a relatively high water content was used to increase the concrete porosity and permeability, which allowed it to act as an effective electrolyte medium during the accelerated corrosion mechanism. The concrete mix design used is presented in Table 1. The water-cement ratio of this mix was 0.75, 20mm aggregates were used, and the anticipated concrete compressive strength  $f'_c$  was 25 MPa. 3% chloride by mass of cement was added to the concrete mix in order to depassivate the reinforcement and initiate the corrosion process.

Table 1. Concrete mix design.

Material	kg/m <sup>3</sup>
Cement	275
Water	205
Coarse aggr.	992
Fine aggr.	838
Total	2310

As the concrete was mixed at the University of Ottawa Concrete Laboratory, a total of 5 batches of 0.12 m<sup>3</sup> each were produced, from which standard concrete cylinder samples were taken for compression tests. The average concrete compressive strength at 7 and 28 days obtained were 21 MPa and 27 MPa, respectively.

In addition to the concrete compressive strength tests, the high-strength non-shrink grout used in the top and bottom steel caps was also tested. At each of the 5 concrete castings, the casting of grout took place before the concrete casting at the bottom of the cylinders and after the concrete casting at the top of the cylinders. Standard cube samples were taken at each grout casting and tested in compression at 7 and 28 days. The average compressive strength of the grout is 53 MPa. Figure 3 shows the formwork used in the production of the column specimens.



Figure 3. Formwork used in the production of the columns.



Figure 4. RC column specimens after formwork removal.

Curing was achieved by using moist burlap fabrics, which in turn were wrapped with plastic sheets to minimize evaporation. The specimens were sprayed with water at least once per day in order to ensure sufficient moist conditions for hydration. The curing regime lasted for 14 days after formwork removal. Figure 4 shows the final columns with top and bottom steel caps.

## 2.2 Sustained loading setup

Two 332×332×38-mm steel plates placed at the top and bottom ends and connected with four 25-mm diameter steel rods were used to keep the columns under a sustained axial compression load. The column itself was mounted between the two steel plates with a central high-strength 16-mm thick circular steel plate, which was fully welded to the square plate but not welded to the column cap plates, in order to simulate an axial pin connection. By subjecting the four steel rods to a tensile force, the RC columns were subjected to a constant axial compressive load. The tension steel rods used to apply the load were also painted with a corrosion resistant primer. A tension force of 55 kN was applied at each rod, with a

total axial compression load of 220 kN on each column. This load represents 30 to 40% of the design axial capacity of the column, simulating in-service conditions.

## 2.3 Accelerated corrosion setup

In order to induce corrosion on the reinforcement, the columns were electrically connected to a PGSTAT100 potentiostat. A constant anodic current density was impressed on the steel reinforcing bars, while four stainless steel sheets (25-mm wide by 400-mm long) were placed directly at the column exterior serving as counter-electrodes. The stainless steel sheets were placed during casting on the wet concrete surface to ensure optimum contact. The reinforcing bars were connected to the electrical wires of the potentiostat by means of welded screws with nuts covered with electrical tape to limit the effects of corrosion at these sensitive points. These connections were also zinc-paint coated for maximum protection. The specimens were further exposed to wetting and drying cycles instead of completely being immersed in water, in order to ensure a sufficient supply of moisture and oxygen for the electrochemical reactions. The wet-dry cycles were applied at constant time intervals with a pump that sprayed water through a perforated hose placed around the columns.

Three out of the five CV specimens (specimens CV1, CV2, and CV3) had their spiral reinforcement isolated from the vertical reinforcement using temperature shrink tube, and the electrical current was applied to the longitudinal reinforcement. For the remaining two specimens under these series, one column (specimen CVG) underwent general corrosion of the entire reinforcement cage, while the other one served as the control (or uncorroded) specimen. Similarly for the CS series, three columns (specimens CS1, CS2, and CS3) had their longitudinal reinforcement isolated from the spiral reinforcement using electric tape, and the electrical current was applied to the reinforcement used for confinement. Specimen CSG underwent general corrosion of the entire reinforcement cage, and the remaining one served as the control specimen for this series. Figure 2 shows how the vertical reinforcement was electrically isolated from the spiral reinforcement by covering the longitudinal reinforcing bars with tape at the contact points.

The PGSTAT100 is a potentiostat that simulates an electrochemical cell with three main electrodes: the working electrode connected to the reinforcing steel, the counter electrode connected to the stainless steel sheets, and the reference electrode that measures the potential. Galvanic-cell electrical current measurements were also taken by the potentiostat in order to monitor the corrosion rate of the RC column

specimens. The current density applied on the specimens ranged between 280 and 315  $\mu\text{A}/\text{cm}^2$ . These current densities are much higher than those recorded in the field (Rodriguez et al. 2000); however, they induce a certain level of damage in a relatively short period of time. Figure 5 shows two specimens in their final setup under load and subjected to accelerated corrosion. In this figure, corrosion staining, which appeared 15 days after the initiation of the accelerated corrosion process, can already be observed at some existing shrinkage cracks on the concrete surface.

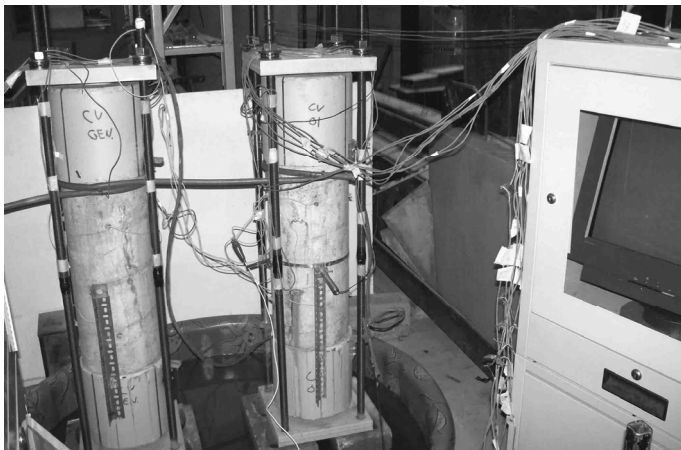


Figure 5. Final load and accelerated corrosion setup.

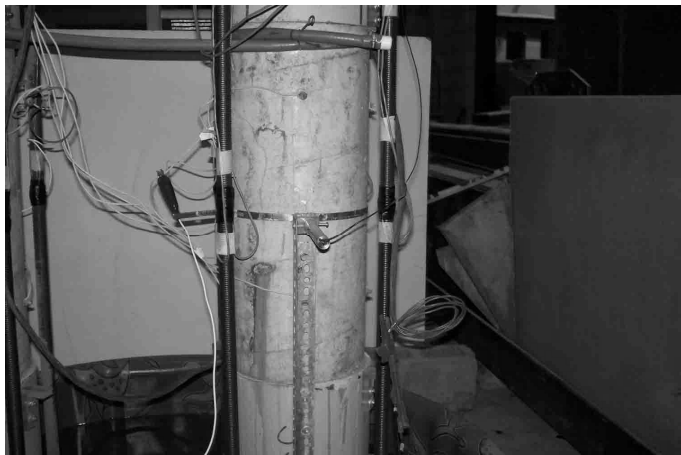


Figure 6. Electrodes and LVDTs of the experimental system.

## 2.4 Strain & deformation

Strain gauges were placed on the steel tension rods in order to monitor the compression load applied to the columns. Each of the four rods had two strain gauges attached at its centre, with a total of 8 strain gauge readings. In addition, three LVDTs were used to monitor the deformation in the columns. Two LVDTs were used vertically to measure the total shortening of the columns as a result of the compressive load, and the remaining LVDT was used horizontally at column mid-height (placed at an expandable circular thin metal sheet wrapped around the column) to measure the circumferential expansion. Figure 6 shows the electrodes, the perforated hose

used to spray water, the strain gauges, and the LVDTs on an RC column specimen.

Strain and deformation measurements were taken at approximately every three weeks with a data-acquisition software. After calibration of the strain readings taken at the steel rods, it was determined that a strain reading of  $730 \times 10^{-6}$  corresponds to 55 kN tension load on the steel rod. The load was therefore adjusted after these measurements to keep it constant at 55 kN at each rod.

## 3 EXPERIMENTAL RESULTS

### 3.1 Crack propagation over time

Cracking in the concrete cover of the RC columns was monitored over the testing period. Once cracking was visually observed, crack widths were measured every two months using feeder blade inserts. The first round of testing lasted for 10 months, and it included the application of accelerated corrosion on column specimens CVG, CV1, CSV, and CS1. The second round of testing lasted only 4 months, and it included column specimens CV2, CV3, CS2, and CS3. Therefore, data for specimens CVG, CV1, CSV, and CS1 goes up to 10 months, while data for specimens CV2, CV3, CS2, and CS3 goes up to 4 months.

In columns type CV, mostly longitudinal cracking along the vertical reinforcement was observed. On the other hand, in columns type CS, the cracking pattern that was observed corresponded to that of smaller and more scattered cracks along the spiral reinforcement. This was expected since the electrical current was applied only to the vertical reinforcement for columns CV, while the electrical current was applied only to the spiral reinforcement for columns CS. Exceptions were columns CVG and CSG, in which the entire reinforcement cage was subjected to an electrical current.

Corrosion damage started to become visible towards the end of the second week of testing for all column specimens. All specimens showed initial discolouring at random spots across the concrete cover surface, with corrosion gel leaking through existing cracks and voids in the concrete. Towards the third week of testing, all column specimens started to show hairline cracks. Specimens type CV showed longitudinal vertical hairline cracking along the location of the vertical reinforcement. By the second month, these cracks had an opening between 0.083 mm and 0.14 mm wide. Figure 7 plots the increase in longitudinal crack widths over time for columns CV. The figure shows the average crack width measured for each specimen. Crack width measurements at areas that appeared to be spalling or almost spalling and were wider than 1 mm are not included



in Figure 7. As observed from the figure, although all specimens experienced an increase in crack widths over time, specimen CVG, whose reinforcement cage was all subjected to accelerated corrosion, displayed the higher values of crack widths after 10 months of exposure.

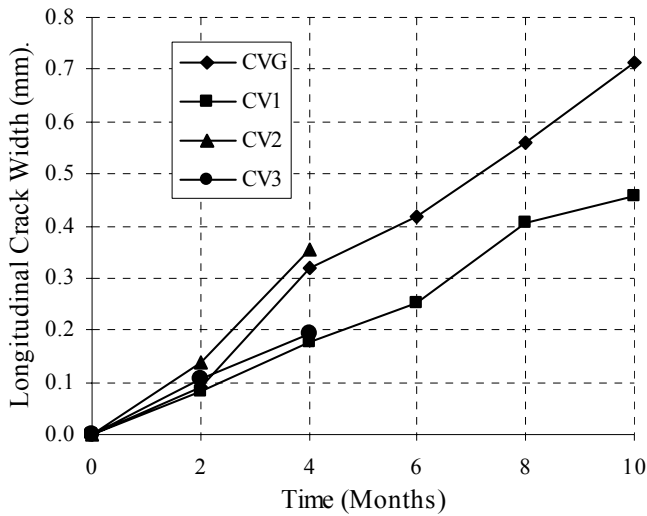


Figure 7. Longitudinal cracking width over time in columns type CV.

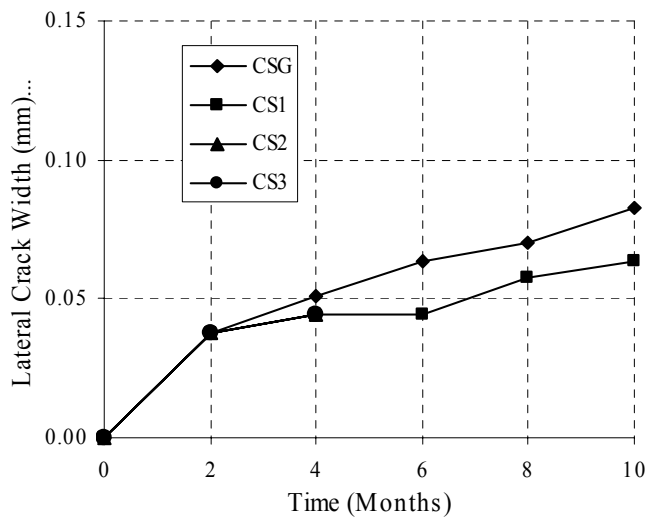


Figure 8. Lateral cracking width over time in columns type CS.

Specimens type CS showed minor hairline cracks going laterally and scattered at various spots across the concrete cover. Although these cracks were continuously leaking corrosion rust product, they were too small and difficult to measure until about the second month of testing. Towards that time, it became possible to insert the 0.038 mm feeder blade in most of the cracks. Figure 8 shows the increase in lateral crack widths over time for columns CS. Figure 8 plots the average crack width obtained for specimens CSG and CS1 for a period of 10 months and for specimens CS2 and CS3 for a period of 4 months. As shown in the figure, these lateral cracks are a lot less wide than the vertical cracks observed

in columns type CV: 0.083 mm was recorded as the maximum lateral crack width for columns type CS as opposed to 0.712 mm as the maximum longitudinal crack width for columns type CV. Figure 9 shows typical surface cracking as observed in these two close-up photos of a longitudinal crack at column CV1 taken at 10 months, and some lateral cracks at column CS3 taken at 4 months.



Figure 9. Cover surface cracking (longitudinal).

### 3.2 Corrosion induced damage

Since concrete cracking is partly due to the rust formation produced by the oxidation of the reinforcement, cracking propagation is considered to be directly related to the loss of reinforcement cross section. The steel mass loss  $M$  due to reinforcement corrosion is related to the electrical current  $I$  through Faraday's law as follows:

$$M = \frac{I \cdot t \cdot A_w}{z \cdot F} \quad [\text{g}] \quad (1)$$

where,  $I$  = current (A);  $t$  = time (s);  $A_w$  = atomic weight (55.85 g/mol);  $z$  = valency, which equals 2; and  $F$  = Faraday's constant (96500 coulombs/equivalent mass). By substituting the corrosion current density  $i$  (electrical current per surface area of rebar) into Equation 1, the diameter reduction  $x(t)$  of the reinforcing bar after time  $t$  can be calculated from:

$$x(t) = \frac{A_w}{z \cdot F \cdot \rho} \cdot i \cdot t \quad (2)$$

where  $\rho$  = density of iron (7.85 g/cm<sup>3</sup>). By substituting the values of  $A_w$ ,  $z$ ,  $F$  and  $\rho$ , and calculating the rate of thickness reduction in mm/yr with  $i$  given in  $\mu\text{A}/\text{cm}^2$ , the following expression results:

$$x(t) = 0.0116 \cdot i \cdot t \quad (3)$$

where  $x(t)$  is given in mm,  $i$  is given in  $\mu\text{A}/\text{cm}^2$ , and  $t$  is given in years.

In this investigation, the potentiostat current applied varied between 280 and 315  $\mu\text{A}$ , which translated into a current density of approximately 100  $\mu\text{A}/\text{cm}^2$  applied to the column specimens. Equation 3 was used to calculate the reduction in the reinforcement diameter over the period of simulated accelerated corrosion. Figure 10 plots the average crack width for each column type relative to the reduction in the rebar diameter due to corrosion. The crack width reported in Figure 10 has been calculated as the average of column specimens CV1, CV2, and CV3, and the average of column specimens CS1, CS2, and CS3 over the 10-month period. The graph shows an approximately linear variation of the crack width for both column types relative to the bar diameter reduction. The theoretical maximum bar reduction was calculated to be 0.322 mm at the end of the 10 months period; this implicitly assumes that all the electrical current was used in the corrosion process and that there were no losses. This reduction in the reinforcement diameter will have to be verified through forensic analysis of the corroded reinforcing bars. It can be seen from Figure 10 that crack widths increase approximately linear with time for both column types. A similar trend has been previously observed by Rodriguez et al. (2000).

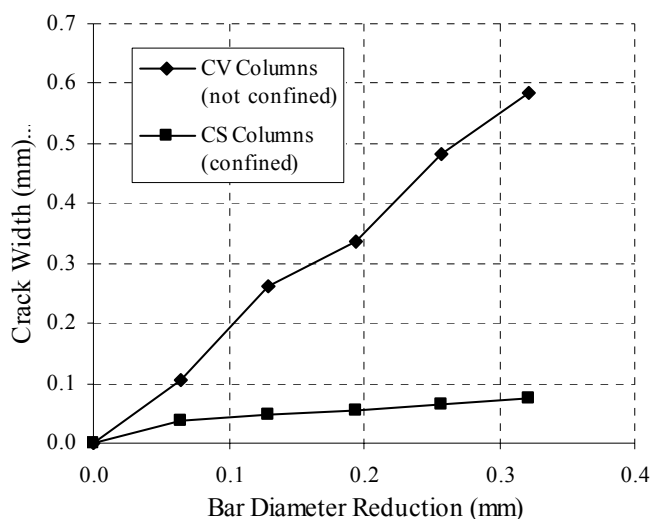


Figure 10. Average crack width versus bar diameter reduction.

### 3.3 Column serviceability

Measurements of the columns' vertical shortening and circumferential expansion were also regularly monitored and recorded through the data acquisition on the LVDTs. Figure 11 shows the average values for the vertical and circumferential deformations in mm during the testing period for columns type CV. From the figure, it can be observed that column CVG, whose entire reinforcement was subjected to corrosion, experienced most of its vertical deforma-

tion in the first two months and stabilized after that, while column CV1 displayed a continuous increase of its axial deformation during the entire testing period. Although columns CV2 and CV3 were only exposed to accelerated corrosion for four months, their rate of column deformation increase is similar to column CV1. The rate of increase of the circumferential expansion was very low for a period of 10 months.

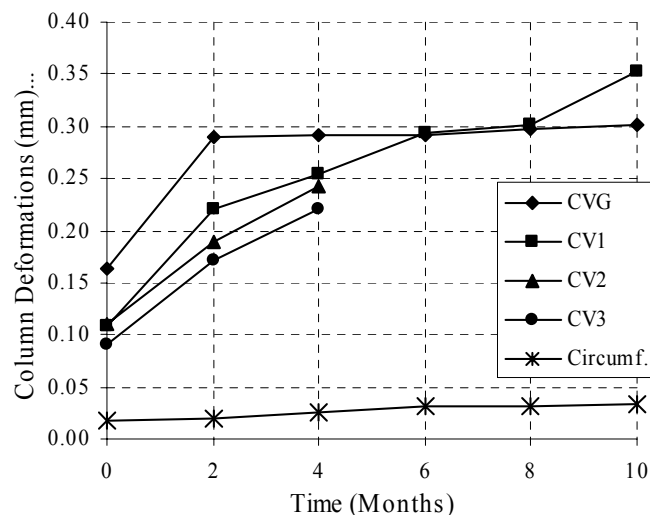


Figure 11. Column deformations over time for columns CV.

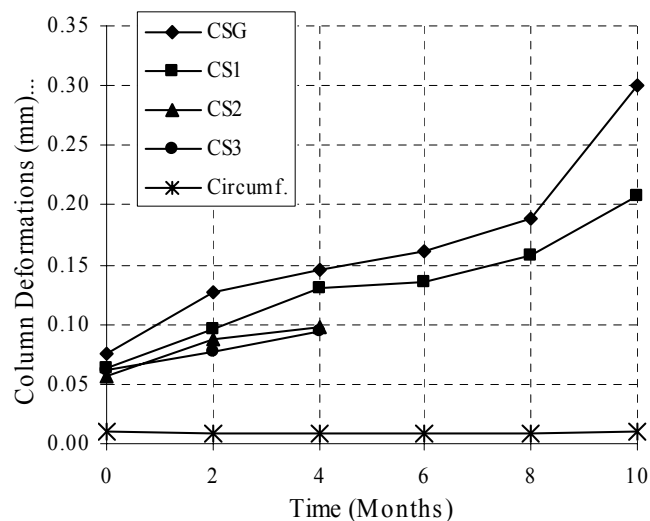


Figure 12. Column deformations over time for columns CS.

It should also be noted that these deformations include the effects of creep and shrinkage of the concrete. Cracking cannot be considered as the primary cause of deformations especially during the initial stages of the testing procedures.

Figure 12 plots the deformations versus time in columns type CS. By comparing Figures 11 and 12, it is observed that deformations in columns CV as well as the rate of their increase over time were higher than columns CS. For the latter group, vertical deformations appear to plateau slightly after 3 months of testing, before they start increasing again

at 8 months. The circumferential expansion was relatively smaller than that of columns CV. In fact, it is concluded from the results that column expansion is further increased as the area of longitudinal reinforcement participating in the resistance of the axial load is decreased due to corrosion.

Figure 13 shows the vertical shortening obtained in mm for both column types versus the crack width. Although deformations obtained for columns CV were higher than those obtained for columns CS, the increase in vertical deformation as a function of crack opening is more pronounced for columns CS. The combined effect of corrosion of spiral reinforcement and concrete cover cracking considerably reduces the confinement action in columns CS. This type of columns require less crack opening to achieve a similar level of axial deformation than columns CV.

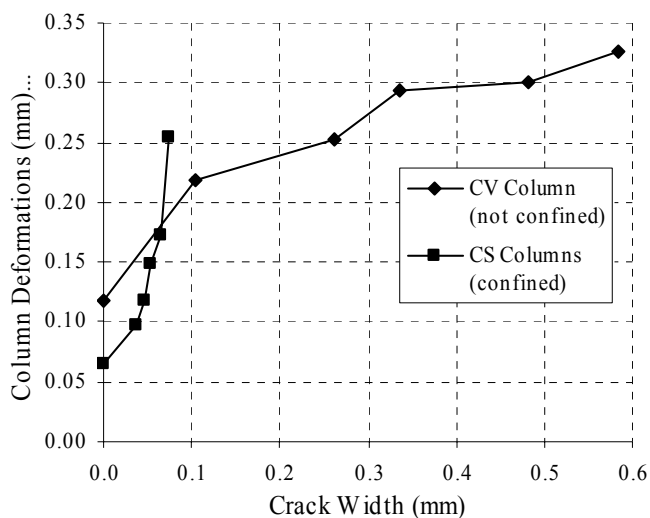


Figure 13. Vertical shortening versus crack width.

## 4 DISCUSSION

### 4.1 Effect of sustained load on crack propagation

Loads were kept constant on the column specimens during the corrosion simulation. This had a significant impact on the lateral crack propagation. Although the reduction in the reinforcing bar diameter for the testing period was similar for both types of columns (see Fig. 10), the lateral crack widths in columns CS were significantly less than the widths of the longitudinal cracks in columns CV. This was most likely due to the vertical pressure of the sustained loading that is in the perpendicular direction to the lateral cracks, unlike the longitudinal cracks that had little counter-pressure. Therefore, in terms of crack width, the effect of corrosion on spiral reinforcement has a less severe impact on cover cracking than the effect of corrosion of vertical reinforcement in a column. The width of the longitudinal cracks

along the vertical bars was approximately 6 to 8 times the width of the lateral cracks. However, the lateral cracks along the spiral ties constitute spots of potential future pitting in the concrete cover.

### 4.2 Effect of wet-dry cycles

The continuous discolouring of the column surface was an indication that the rust products were being constantly washed away and dissolved in water through the cracks. Perhaps a method of moisture supply different from spraying with water such as humidity or fog chamber would have a different impact on cover cracking. Not allowing the rust product to dissolve in the water might lead to further accumulation around the rebar surface and more severe cracking in the concrete.

### 4.3 Effect of cover cracking on column serviceability

Results show that the effect of cover cracking up to the corrosion levels investigated have an impact on the column serviceability, particularly due to the increase in the columns vertical deformations towards the second half of the ten months of corrosion testing. This clearly shows that further column deterioration in the form of cover cracking is an indication of a reduction in the column structural performance in regards to serviceability criteria.

## 5 CONCLUSIONS

This paper has presented experimental results related to concrete cracking and longitudinal and lateral deformations of RC circular columns that were simultaneously subjected to axial load and accelerated reinforcement corrosion. While in one set of columns only the longitudinal reinforcement was subjected to corrosion, in the other set of columns it was the spiral reinforcement designed to provide column confinement that was corroded. The cracking pattern observed was quite different for the two sets of columns. Columns whose longitudinal reinforcement was corroded exhibited vertical cracking parallel to the longitudinal reinforcing bars. On the other hand, columns whose spiral reinforcement was corroded displayed a more random cracking pattern distributed in the lateral direction. In general, columns whose longitudinal reinforcement suffered from corrosion experienced higher axial and lateral deformations, and the associated crack widths were six to eight times higher in magnitude than the other set of columns. This experimental study will be completed with testing the column specimens up to failure by subjecting them to eccentric axial loading.

## REFERENCES

- Andrade, C. & Alonso, C. 1996. Progress on design and residual life calculation with regard to rebar corrosion of reinforced concrete. In N.S. Berke, E. Escalante, C.K. Nmai & D. Whiting (eds), *Techniques to Assess the Corrosion Activity of Steel Reinforced Concrete Structures, ASTM STP 1276*: 23-40.
- Lee, C., Bonacci, J.F., Thomas, M.D.A., Maalej, M., Khajepour, S., Hearn, N., Pantazopoulou, S., & Sheikh, S. 2000. Accelerated corrosion and repair of reinforced concrete columns using carbon fibre reinforced polymer sheets. *Canadian Journal of Civil Engineering* 27(5): 941-948.
- Liu Y. & Weyers R.E. 1998. Modeling the time-to-corrosion cracking in chloride contaminated reinforcement concrete structures. *ACI Materials Journal* 95(6): 675-681.
- Rodríguez, J., Ortega, L. M., & Aragoncillo, J. 2000. Corrosion rate and structural performance. In C. Andrade, C. Alonso, J. Fullea, J. Polimon, & J. Rodríguez (eds), *Measurement and Interpretation of the On-site Corrosion Rate*: 191-213. RILEM Publications S.A.R.L.
- Rodríguez, J., Ortega, L. M., & Casal, J. 1996. Load bearing capacity of concrete columns with corroded reinforcement. In C. L. Page, J.W. Figg, & P.B. Bamforth (eds), *Corrosion of Reinforcement in Concrete Construction*: 220-230. Royal Society of Chemistry.
- Saito, Y., Michiaki, O., Kanakubo, T., & Yamamoto, Y. 2007. Structural performance of corroded RC column under uniaxial compression load. *First International Workshop on Performance, Protection & Strengthening of Structures under Extreme Loading*, Whistler, Canada.

acknowledgments

Financial support provided by the Natural Sciences and Engineering Research Council of Canada, and by Halsall Associates Limited is gratefully acknowledged.